PHYSICAL REVIEW VOLUME 70, NUMBERS 9 AND 10 NOVEMBER 1 AND 15, 1946

The Orientation of Electrical Breakdown Paths in Single Crystals

J. W. DAVISSON*
Laboratory for Insulation Research, Massachusetts Institute of Technology, Cambridge, Massachusetts
(Received July 8, 1946)

The effect of temperature on the orientation of electrical breakdown paths in the alkali halide crystals has been investigated. The results obtained suggest the existence of a path sequence

random→[100]→[111]→[110]→[*xxy*]

assumed by the direction of breakdown as the lattice energy or temperature increases. Star patterns of 12 non-primitive lattice directions were observed in LiCl and LiF. Mixed and impure crystals grown from the melt tend to exhibit high temperature path patterns at low temperatures. By extending the study at room temperature to crystals possessing different bonding and symmetry properties, general laws governing path orientation are established. It is shown that the possible path directions depend upon the macroscopic symmetry prevailing and are apparently not influenced by the type of lattice bond.

I. INTRODUCTION

THAT electrical breakdown through single crystals can result in the formation of breakdown paths orientated in distinct crystallographic directions was discovered independently and almost simultaneously by L. Inge,[1] A. von Hippel,[2] and J. Lass.[3] A comprehensive survey of the phenomenon in the alkali halide crystals by von Hippel,[4] using homogeneous and inhomogeneous fields, gave direction laws as partly summarized in Table I. In NaCl at room temperature, for instance, with the field orientated in the [100] direction, the paths proceeded from the anode in the [110] direction, but were apt to change to [111] before reaching the cathode, thus forming characteristic tetrahedral pyramids resting with their bases on the cathode plane (Fig. 1).

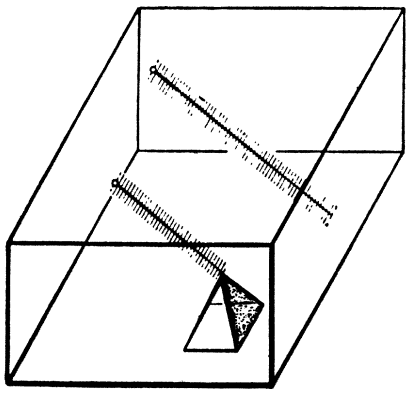

FIG. 1. Breakdown of NaCl (paths starting at the anode in the [110] direction and splitting near the cathode into [111] paths).

It was also found that the direction laws for breakdown through the volume of the crystal reappear in the direction which discharge paths may take on its surface,[4] and that addition agents influence the selection of path directions in the volume and surface breakdown in a similar manner.[5] Surface patterns on less symmetrical crystals have been observed by Kreft and Steinmetz.[6]

TABLE I. Appearance and direction of the breakdown path in the alkali-halide crystals.

Crystal	Appearance	Direction (the field direction is [100])
LiF, NaF, NaCl	sharp	primary [110], secondary [111]
KCl, RbCl	sharp	[110] and [100]
NaBr	a little blurred	[110], but also [111], [100] and random
KBr, KI, RbBr, RbI	blurred	[100] and random

* This communication is an abstract of a thesis submitted (1943) in partial fulfillment of the requirements for the degree of Doctor of Philosophy in Physics at the Massachusetts Institute of Technology.

[1] L. Inge and A. Walther, Zeits. f. Physik **64**, 830 (1930); **71**, 627 (1931).

[2] A. von Hippel, Zeits. f. Physik **67**, 707 (1931); **68**, 309 (1931).

[3] J. Lass, Zeits. f. Physik **69**, 313 (1931).

[4] A. von Hippel, Zeits. f. Physik **75**, 145 (1932); Ergeb. d. exakt. Naturwiss. **14**, 104 (1935); J. App. Phys. **8**, 815 (1937).

[5] A. von Hippel, Zeits. f. Physik **88**, 364 (1934).

[6] F. Kreft and H. Steinmetz, Zeits. f. angew. Min. **1**, 144 (1937). H. Steinmetz, Naturwiss. **22**, 314 (1934).

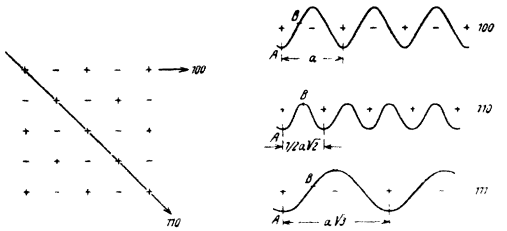

FIG. 2. Potential structure of NaCl.

If breakdown is initiated at the cathode, the path orientation is not the same as in the anodic phenomenon; thus [100] instead of [110] paths are formed in NaCl at room temperature.[1–3]

Metallic dendrites (of Na metal in NaCl crystals, etc.) may be grown from the cathode in the alkali halide crystals at elevated temperatures and show again characteristic crystallographic orientations.[7]

By measuring the breakdown strength of the alkali halides quantitatively, von Hippel[4] was able to formulate a tentative theory of the breakdown process. This assumes that excess electrons, produced by some ionizing process or introduced into the structure from the outside, are accelerated by the applied field after overcoming the friction barrier of the lattice vibrations, and produce impact ionization, avalanche formation, and breakdown. The direction laws follow from the assumption that the electrons take the paths offering the least friction, and that these paths are determined by the potential structure of the material. For NaCl the [110] direction offers the lowest potential barriers (Fig. 2), the [111] direction the flattest potential modulation and smallest number of ions per unit length of path, while the [100] direction is most unfavorable in both respects.

A difficulty arose when the breakdown strength of NaCl was measured as a function of the orientation of the crystal relative to the field.[8] No dependence of the strength on orientation was found. This suggested that in traversing the maximum of the vibration barrier the electrons are still moving so slowly that their long wavelength makes it impossible for them to discern the lattice structure; only after sufficient acceleration will the electrons move in selective directions. This fact made it very doubtful that the potential structure was a decisive factor in determining the breakdown direction, because the electrons were apparently able to cross the potential barriers in all directions without noticing their existence. Consequently, the research here reported was undertaken to obtain more information concerning the mechanism of path formation.

[7] A. von Hippel, Zeits. f. Physik **98**, 580 (1936).
[8] A. von Hippel and J. W. Davisson, Phys. Rev. **57**, 156 (1940).

II. APPARATUS AND PROCEDURE

The simplest and most satisfactory device used to produce breakdown paths was an ordinary leak-tester such as is commonly used in testing vacuum systems.[4]

A section (about $\frac{1}{4}$ cm thick) of crystal to be treated was placed on a metallic plate in the bottom of a vessel filled with a suitable insulating medium with the tester in contact with the upper surface. The insulating medium prevented the spark discharge from taking place in the air or over the surface of the crystal. Breakdown paths at different temperatures were obtained by using the following insulating media: (1) liquid air, (2) dry ice and butanol, (3) transformer oil, (4) transformer oil heated to 200°C, (5) boiling sulphur, and (6) electrical heating inside a vacuum.

Since the tester provided an alternating positive and negative voltage of unknown magnitude, the path orientations were checked in several cases by means of a steady d.c. voltage by using ivory electrodes.[4] The ivory electrode sample holder consisted of two highly polished and slightly rounded ivory electrodes between which a thin (2- to 8-mil) section was placed. The system was inserted in a bomb containing nitrogen at 100 atmospheres to suppress corona, and a steady d.c. voltage from a suitably filtered power source was applied. The ivory electrodes provided a homogeneous field across the sample and limited the current at breakdown so that secondary destruction did not obliterate initial breakdown effects.

In most instances the path directions obtained by the two methods were identical, i.e., in sulphur, baryte, aragonite, calcite, fluorite, sphalerite, and the majority of the alkali halides. The peculiar breakdown obtained in fluorite at room temperature (V, 1, B), however, was obtained

only with the leak-tester in thick samples. It should be remarked that breakdown paths are characteristically an inhomogeneous field phenomenon, since the positive space charge existing along the path channels acts as an auxiliary electrode that renders the field inhomogeneous within the crystal even when homogeneous fields are applied.[4]

The tester, in addition to its convenience in allowing the use of thick samples and a simple method of temperature control, also permitted visual observation of path formation so that intricate patterns could be grown without actual failure through the sample taking place. The path growth could also be halted or made to progress very slowly, thus, the effect of weak and strong fields upon path orientation could be studied in detail.

The patterns obtained by the above methods were examined under the microscope and the angular coordinates of the paths θ, φ measured. The inclination angle θ was measured against the nomal to the section, and the azimuthal angle φ between the horizontal path projection and a "datum line" on the surface. In Fig. 3 the lower diagram represents a crystal section of orientation (hkl) whose unit normal is represented in the unit sphere of the upper diagram by the vector n. The dotted vector in the crystal, represented by n_2, is a unit vector in the direction of the breakdown path. n_3 is directed along the surface projection of the path, and n_1 is a unit vector directed along the "datum line" which is usually parallel to a crystal edge. φ is the angle between n_1 and n_3, and θ is the acute angle between n and n_2.

The angular coordinates θ, φ were transformed into zonal parameters $[uvw]$, which are components of the path directions upon the crystallographic axes, and thus the path directions could be correlated with symmetry properties and atomic structure of the crystal. The zonal parameters $[uvw]$ are related to the Miller indices (hkl) and to the unit cell through the expression

$$H=ua_1+va_2+wa_3=hb_1+kb_2+lb_3,$$

where H is any vector direction, the a vectors are unitary lattice vectors defining the unit cell, and the b vectors are the associated reciprocal unitary lattice vectors. The transformation equations for θ, $\varphi \rightarrow [uvw]$ may be represented (Fig. 3) by

$$n_1 \cdot n_2 = \cos\varphi \sin\theta,$$
$$n \cdot n_2 \times n_1 = \sin\varphi \sin\theta,$$

where n_1 (the datum line)

$$= u_1a_1+v_1a_2+w_1a_3/|u_1a_1+v_1a_2+w_1a_3| \text{ etc.}$$

The above equations may be expanded in each crystal system to yield the transformation equations desired.

In the isometric (cubic) system the direction $[hkl]$ is always normal to the plane (hkl).

According to the laws of crystal symmetry a direction $[uvw]$ is a member of a set of equivalent directions $[[uvw]]$ which can be derived from the first one by macroscopic symmetry operations.[9] By analyzing the path patterns observed the extent to which the path directions conform to one or more sets of equivalent directions was investigated.

III. BREAKDOWN PATHS IN THE ALKALI HALIDE CRYSTALS*

1. Rubidium and Potassium Halides

As Table III shows, the rubidium and potassium halides exhibit the following transitions in their breakdown path patterns as the temperature increases:

$$\text{random} \rightarrow [100] \rightarrow [110].$$

Thus, at liquid air temperature, for KBr, KI, RbBr, and RbI the paths are without orientation and resemble breakdown paths in amorphous media. As the temperature is raised, first [100] paths form and at more elevated temperatures [110] companion paths appear. Figures 4 and 5 illustrate the transition from random at -180°C to [100] at 20°C in RbBr.

In RbCl at -180°C random paths exhibit a strong tendency to orientate in the [100] directions, and KCl exhibits complete [100] orienta-

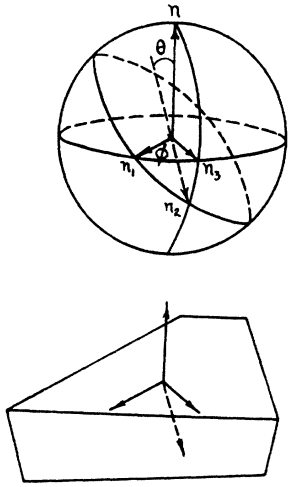

FIG. 3. Breakdown path coordinates.

[9] See Davey, *Crystal Structure and its Applications*, International Series in Physics (McGraw-Hill Book Company, Inc., New York, 1934).

* The alkali halide crystals prepared for this investigation were grown from the melt by the Kyropoulos method. (S. Kyropoulos, Zeits. f. Anorg. u. angew Chemie **154**, 308 (1926).) LiF crystals were obtained from the Harshaw Chemical Company, Cleveland, Ohio.

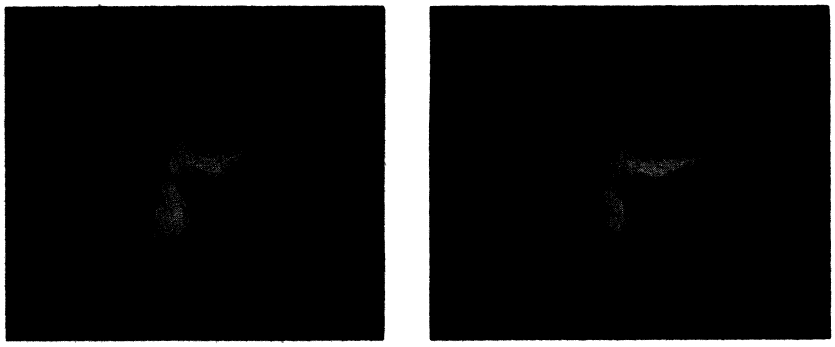

FIG. 4. Random RbBr −180°C.

tion at −180°C. Thus increase of lattice energy tends to influence the path patterns in the same way as increase of temperature.

2. Sodium Halides

The sodium salts exhibit the same type of thermal dependence of path orientation as shown by the rubidium and potassium halides. In addition, however, [111] paths are observed which, on the basis of inconclusive evidence, seem to belong between [100] and [110]. The tentative path sequence is

$$\text{random}\rightarrow[100]\rightarrow[111]\rightarrow[110].$$

The individual salts behave as follows:

A. Sodium Bromide

a. 20°C—random paths (see, however, Table I).

b. 150°C—[111] paths transforming into [110] in regions of weak field strength; [110] paths dominant.

c. 500°C—[110] dominant; [111] not observed.

B. Sodium Chloride

a. Liquid air temperature—

pure NaCl—random paths favoring the [100] directions for all orientations of the crystal (Fig. 6). The [100] orientation tendency seems to be more pronounced in strong than in weak fields.
thin sections of pure NaCl subjected to overvoltage—[100] paths usually accompanied by fractures (Fig. 7).
thin sections of mixed (NaCl+4.6 mole percent AgCl) crystals subjected to overvoltage—sharp [110] paths accompanied by (110) fracture planes.
mixed (NaCl+1 mole percent AgCl) crystals—sharp [100] and [110] paths.

b. Room temperature—

pure NaCl—sharp [110] paths (Fig. 8) for all orientations of crystal.
thin sections pure NaCl subjected to overvoltage—sharp [111] paths usually accompanied by factures (Fig. 9).
mixed (NaCl+AgCl) crystals—precise [110] paths.
cathodic breakdown in (100) and (110) sections of pure NaCl takes place in the [100] direction.

c. At 500°C—precise [110] breakdown paths in all samples of pure and mixed crystals. The patterns form with greater facility than at room temperature so that elaborate constructions involving secondary and tertiary branch paths are formed.

d. At 800°C—[110] breakdown paths in precise orientation apparently form up to the melting point.

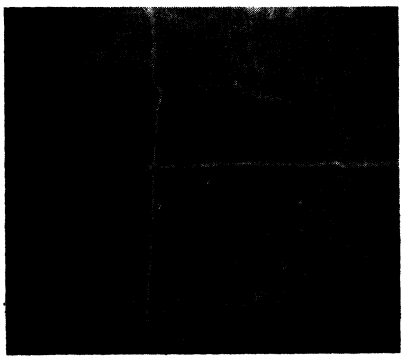

FIG. 5. [100] (100) RbBr 20°C.

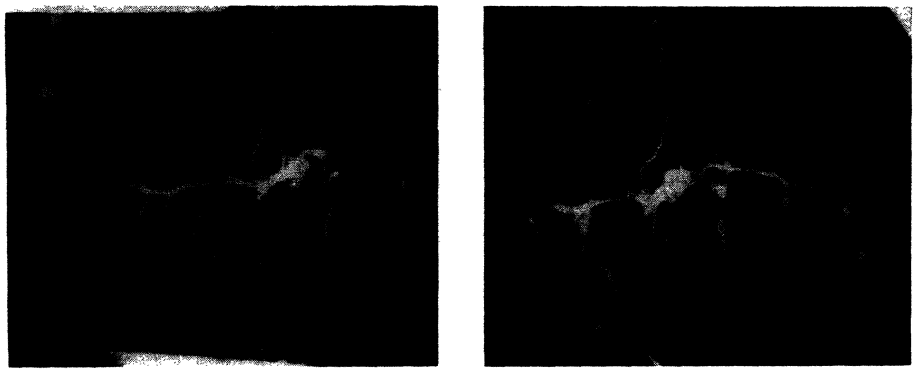

FIG. 6. [100] & R in (110) NaCl at −180°C.

C. Sodium Fluoride

a. At −180°C—sharp [111] paths.

b. At 200°C—[111] paths dominant with [110] companion paths.

3. Lithium Halides

The high temperature path pattern of the lithium salts examined is a temperature dependent 'star' formed by 12 equivalent paths in the non-primitive directions [xxy]. The projection of the 'star' observed in LiCl upon a cube face is shown in Fig. 10. In this design a path projection exists for every 22½° except in the directions of the cube edges. The paths which project into the 45° diagonals have an inclination that is different from the others. In the general case, since the parameters are temperature dependent, the projection figure will not be quite as regular. The 45° projection lines will not change though the inclination of the corresponding paths will. The non-diagonal lines will all be shifted equally toward or away from the diagonals.

FIG. 7. [100] thin (100) NaCl at −180°C overvoltage.

The low temperature pattern in these salts is [110], hence the thermal transitions observed may be represented by

$$[110] \leftrightharpoons [xxy]_T.$$

The individual salts behave as follows:

*A. Lithium Chloride**

a. At −180°C—indications of [110] and star path formation.

b. At 20°C and at 500°C—the star pattern [552] in sharp orientation (Fig. 10).

B. Lithium Fluoride

a. At −180°C—sharp [110] paths.

b. At 20°C—[110] and star paths occur together.

c. At elevated temperatures—the star pattern alone appears and, as Table II shows, the parameters are temperature dependent. Thus at 150°C the pattern (Fig. 11) is accurately represented by the parameters [133] and at 450°C approximately by [122].

It should be remarked that the patterns above are reproducible at least to the extent that in a single experiment the same path directions are obtained from any portion of the crystal surface.

IV. DISCUSSION OF THE ALKALI HALIDE EXPERIMENTS

The breakdown path orientation observed in the alkali halide crystals fall, according to the

* The lithium chloride crystal became contaminated by a speck of rust that fell into the melt during growth.

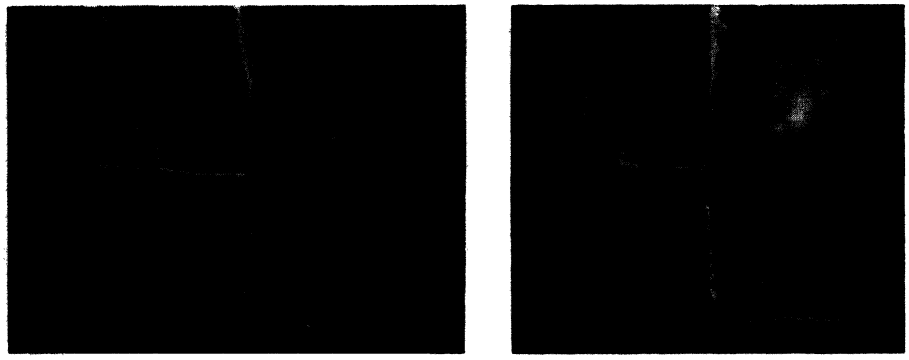

FIG. 8. [110] (100) NaCl 20°C.

data just presented, into the general sequence

$$\text{random} \leftrightarrows [100] \leftrightarrows [111] \leftrightarrows [110] \leftrightarrows [xxy],$$

where Fig. 12,

[100] = 3 equivalent cube-edge directions,
[111] = 4 equivalent body-diagonal directions,
[110] = 6 equivalent face-diagonal directions,
[xxy] = 12 equivalent non-primitive directions such that two components are equal.

The position of the [111] paths in the sequence above is uncertain, since they were never observed in the potassium or rubidium halides (Table III). In NaF, however, [111] paths appear alone at −180°C, and dominant [111] with [110] companion paths appear at elevated temperatures (III, 2, C).

Change of temperature of an alkali halide crystal influences breakdown paths in three ways: it (*a*) affects the rigor of orientation, (*b*) influences the tendency to form branch paths, (*c*) allows patterns of different orientation to appear.

The orientation of the paths becomes more rigorous, and the tendency to form branch paths increases with increase of temperature. Paths in precise orientation apparently form up to the melting point of the crystal.

The influence of temperature upon breakdown path orientation is summarized in Table III where it will be noted that the transition from one dominant path orientation to the next takes place gradually over a temperature range of several hundred degrees. Increase of temperature favors transitions to the right in the sequence above.

Increase of lattice energy, as shown by Table IV, acts in the same sense as increasing the temperature. It should be noted, however, that [111] paths were observed only in sodium salts and [xxy] paths only in lithium salts; thus the path directions may also be conditioned by the nature of the ions. It would be of interest to

FIG. 9. [111] thin (100) NaCl at 20°C overvoltages.

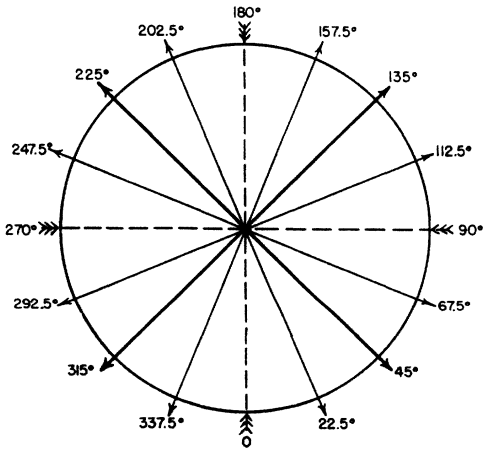

FIG. 10. Projection on the (100) plane of the 12 path star pattern in LiCl.

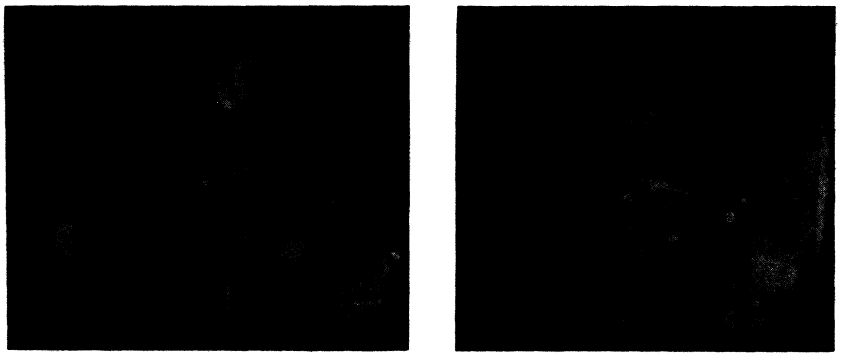

FIG. 11. [133] star LiF 150°C.

examine the patterns in LiI (Table IV), since a star pattern would not be expected if lattice energy is decisive.

Addition agents influence the pattern sequence in the same sense as increase of temperature. Thus, although pure NaCl at −180°C yields random paths favoring the [100] direction, the mixed NaCl+4.6 mole percent AgCl crystal exhibits precise [110] paths at all temperatures investigated. When less AgCl is admitted to the lattice, precise [100] and [110] paths are formed at −180°C, while at elevated temperatures only [110] paths are observed. Iron contamination in LiCl seems to have shifted the path pattern at lower temperatures from [110] to [xxy].

The type of applied voltage also influences the selection of the patterns. Thus in thick sections of pure NaCl at room temperature, [110] paths and not [111] paths are obtained with the tester (Fig. 8); but in thin (1-mil) sections, however, [110] or [111] paths may be produced at will depending upon whether an overvoltage is applied or not. With overvoltage, [111] paths are always formed (Fig. 9). With ivory electrodes [110] and [111] paths are observed in thick sections, but the [111] paths as shown in Fig. 1 tend to form near the cathode plane as branches from [110] paths. At −180°C random paths favoring the [100] directions are observed in thick sections of pure NaCl for all orientations of the crystal (Fig. 6), and in thin (100) sections [100] paths are observed when overvoltage is applied (Fig. 7). In the mixed (NaCl+AgCl) crystals at −180°C, [110] paths are observed when overvoltage is applied to thin sections. With a negative point electrode [100] paths are formed in NaCl at room temperature. These results confirm von Hippel's contention that [111] paths are favored in excess fields in NaCl at room temperature, and show further that the favored direction is temperature dependent, since [100] and not [111] paths are formed at −180°C. A tentative conclusion is that excess

TABLE II. Star path patterns in lithium fluoride. φ_0 observed azimuthal angle against cube edge; φ_c calculated azimuthal angle; θ_0 observed inclination angle; θ_c calculated inclination angle.

[133] pattern at 150°C				[122] pattern at 450°C			
φ_0	φ_c	θ_0	θ_c	φ_0	φ_c	θ_0	θ_c
18.7	18.5	47.3	46.6	28.0	26.6	50.1	48.3
71.0	71.5	45.3	46.6	64.0	63.4	47.2	48.3
109.5	108.5	46.7	46.6	115.5	116.6	47.2	48.3
198.5	198.5	47.7	46.6	134.0	135.0	71.5	71.6
251.5	251.5	48.2	46.6	154.0	153.4	46.7	48.3
288.5	288.5	47.6	46.6	207.0	206.6	50.5	48.3
341.5	341.5	47.2	46.6	224.0	225.0	70.0	71.6
				316.0	315.0	70.3	71.6
				335.0	333.4	47.7	48.3

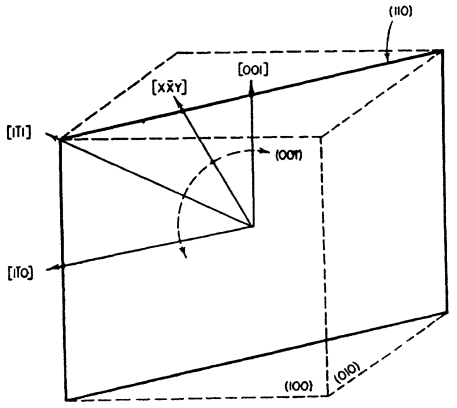

FIG. 12. Directions assumed by breakdown paths in the alkali halides.

TABLE III. Breakdown path orientation in alkali-halide crystals.*

	T°C	F	Cl	Br	I
Li	−180	110	?		
	20	110 & *xxy*	552		
	200	133	552		
	450	122	552		
Na	−180	111	100 & *R*	*R*	
	20	111 & 110	110 & 111	*R* & 100, 111, 110	
	200	110 & 111	110	110 & 111	
	450		110	110	
K	−180		100	*R*	*R*
	20		100	100	*R*
	200		100 & 110	100	100 & *R*
	450		110 & 100	100 & 110	
Rb	−180		100 & *R*	*R*	*R*
	20		100 & 110	100	*R*
	200		100 & 110	100 & 110	100
	450			100 & 110	100 & 110

* The symbol *R* stands for random paths, i.e., without orientation.

fields tend to shift the pattern observed to lower temperature forms. A definite field influence has been observed only in sodium salts.

V. BREAKDOWN PATHS IN CRYSTALS OF DIFFERENT SYMMETRIES

1. Isometric (cubic) System*

A. Periclase (MgO) '32; O_h' [[110]]

Periclase possesses an NaCl structure and a lattice energy of 940 kg cal./mole, as compared with 240 kg cal./mole for LiF.[10] Patterns of the type [*xxy*] or [*xyz*] might, therefore, be anticipated (Table IV), but up to 500°C from (100) faces [110] paths only were observed.

B. Fluorite (CaF_2) '32; O_h' [[110]]

Observations on (111) fluorite are in complete accord with those of Kreft and Steinmetz.[6] At room temperature, although [110] paths develop from the point electrode of the tester, the actual failure of the sample usually takes place abruptly with the formation of a single winding and deviating, unorientated channel that is free from accompanying crystal fractures. This behavior occurred in several different samples that ranged in color from deep violet to clear amber. At elevated temperatures, breakdown paths form more readily and failure takes place in the [110] breakdown path direction. In thin sections, with ivory electrodes, failure in the [110] direction takes place at room temperature, and elaborate [110] surface patterns are sometimes formed. (Fig. 13.)

* The 32 symmetry classes are grouped into 7 systems as follows: 1–2 triclinic; 3–5, monoclinic; 6–8, orthorhombic; 9–15, tetragonal; 16–20, trigonal; 21–27, hexagonal; 28–32, cubic. The symmetry increases with the number; thus, No. 27 denotes the most symmetrical form of hexagonal crystal, etc. The class number together with the familiar Schönflies symbol, which represents the symmetry elements present, is included after the name and formula of the crystal. This is followed by a representation of the path parameters which are enclosed in double brackets to signify that the complete pattern is present.

[10] F. Seitz, *Modern Theory of Solids* (McGraw-Hill Book Company, Inc., New York, 1940), p. 88.

TABLE IV. Breakdown paths in relation to electrical and thermal properties, where U = lattice energy in kg cal./mole—Seitz, *Modern Theory of Solids*, p. 80; E_m = maximum breakdown strength × $(10)^6$ volts/cm—von Hippel (reference 4); $h\nu$ = Reststrahl × $(10)^{-2}$ volt—von Hippel (reference 4). The dash under the path parameter indicates the dominant pattern at room temperature.

Salt	U	E_m	$h\nu$	Path patterns observed			
LiF	240	4.0	7.2			110	*xxy*
NaF	215	2.4	3.3		111	110	
LiCl	193						*xxy*
KF	190		3.0				
LiBr	183						
NaCl	180	1.6	2.4	100	111	110	
NaBr	172	0.8	1.8	*R*	111	110	
LiI	171						
KCl	164	1.0	1.9	100		110	
RbCl	159	0.8	1.7	*R*	100	110	
KBr	158	0.7	1.5	*R*	100	110	
RbBr	152	0.6	1.15	*R*	100	110	
RbI	144	0.5	1.05	*R*	100	110	

C. Sphalerite (ZnS) '31; T_d' [[110]]

In sphalerite the Zn and S atoms are each arranged in face-centered lattices in such a way that a diamond structure would result, if all the atoms were the same. [110] breakdown paths developed in (100) and (110) sections. No temperature effects were noted.

D. Sodium Chlorate ($NaClO_3$) '28; T' [[552]]

This crystal type contains no reflection planes or center of symmetry. The path pattern, which has been described by Kreft and Steinmetz,[6] is identical with [552] star pattern observed in LiCl (Fig. 10). The same pattern was obtained in liquid air and at 200°C.

2. Tetragonal System

A. Apophyllite ($KCa_4(Si_2O_3)\cdot 8H_2O$) '15; D_{4h}' [[110]]

Apophyllite was chosen for investigation because it is a crystallographically symmetrical

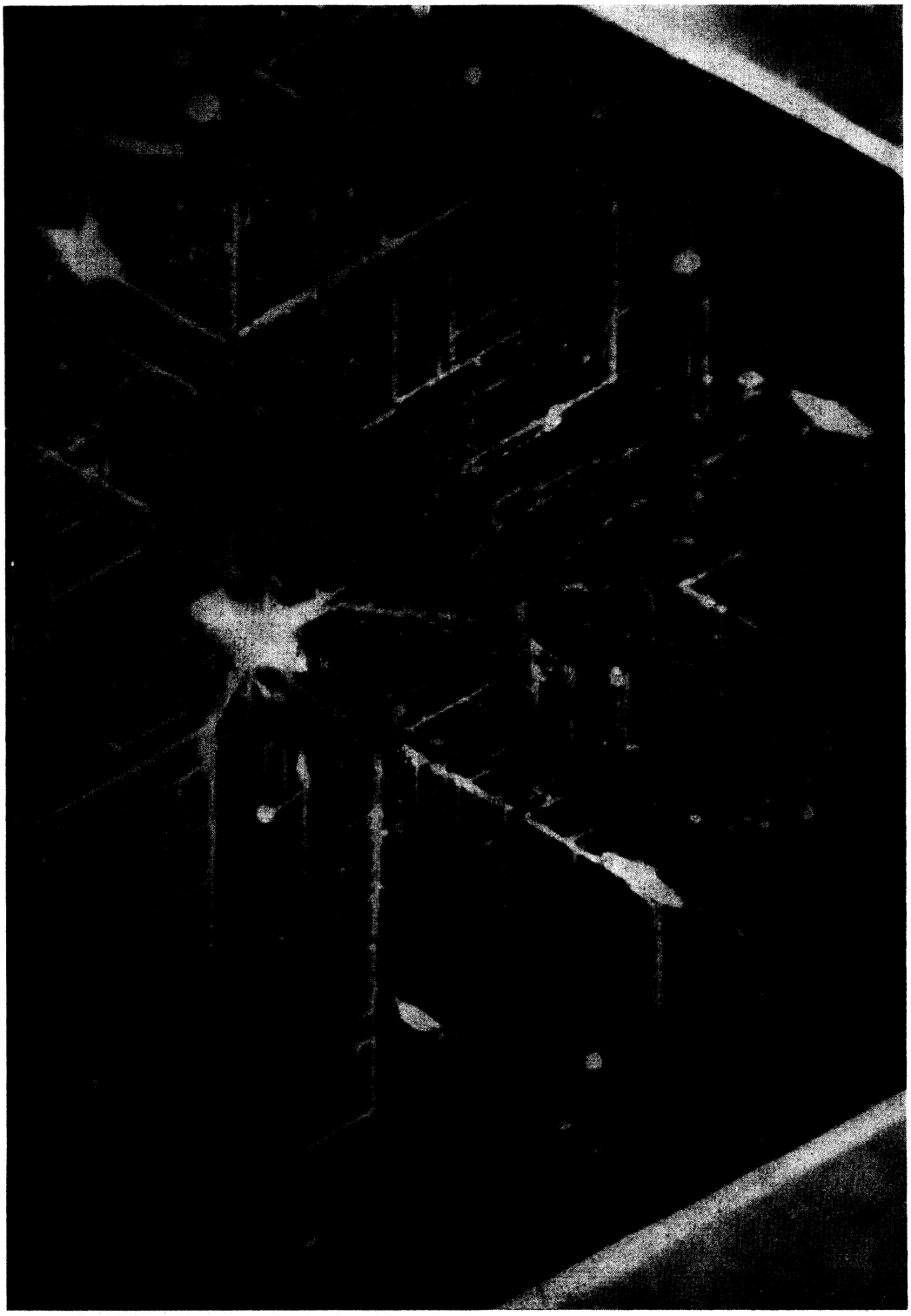

FIG. 13. [110] surface breakdown paths on (111) fluorite.

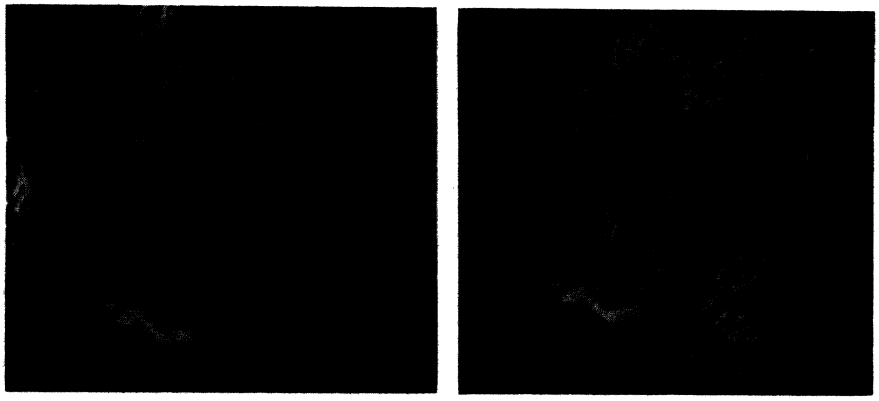

FIG. 14. Pattern in (100) KH_2PO_4.

crystal possessing a complex and distorted atomic structure. It has been described as a distorted layer lattice consisting of alternating puckered silicate rings of 4 and 8 silicon atoms per ring, respectively.[11]

The paths observed in apophyllite are of a simple degenerate nature.

In a (100) section—symmetrical forks lying in the basal (001) plane and inclining at 45°.
In a (010) section—complimentary forks in the (001) plane.
In a (001) section—[001] paths straight through sample.
In a (111) section—the three directions above and no others appear.

The complete pattern, therefore, consists of the paths:

$$[110] \quad [1\bar{1}0] \quad [001]$$

TABLE V. The path pattern of potassium dihydrogen phosphate.

[uvw]	θ calculated	φ	θ observed	φ
20, 9, 16	41.1	329	41.5	328
$\bar{2}0$, $\bar{9}$, 16	41.1	149	41.6	149
$\bar{9}$, 20, 16	70.1	307	70.2	307
9, $\bar{2}0$, 16	70.1	127	70.2	129
15, 4, 7	26.9	33	26.8	33
$\bar{1}5$, $\bar{4}$, 7	26.9	213	27.7	213
$\bar{4}$, 15, 7	76.2	66	74.1	67
4, $\bar{1}5$, 7	76.2	246	76.2	246

[11] W. H. Taylor and St. Naray, Szabo. Zeits. f. Krist. **77**, 150 (1931); Bragg, *Atomic Structure of Minerals* (Cornell University Press, Cornell, New York, 1937), p. 26.

B. Potassium dihydrogen phosphate (KH_2PO_4) *'11; V_d'* [[20, 9, 16]] [[15, 4, 7]]

Since there are only four equivalent points associated with this crystal, and eight path directions were observed, it follows that two sets of patterns are present at room temperature as Table V show. (Fig. 14).

3. Hexagonal System

A. Beryl ($Be_3Al_2(SiO_3)_6$) *'27; D_{6h}'* [[100]], [[001]]

In beryl the breakdown paths are observed to lie along the coordinate axes at room temperature. No change in the pattern was observed at 500°C.

B. Apatite ($Ca_5F(PO_4)_3$) *'25; C_{6h}'* [[9, 14, 11]]

The observed and calculated angles for the path directions are shown in Table VI. The [5, 9, 11] paths do not appear because they possess large inclination angles.

4. Trigonal System

A. Calcite ($CaCO_3$) *'20; D_{3d}'* [[2, 1, 1.45]] [[10, 5, 2]] [[001]]

The observations of Kreft and Steinmetz[6] are confirmed. In basal sections the paths proceed

TABLE VI. The path pattern of apatite.

[uvw]	θ calculated	φ	θ observed	φ
9, 14, $\bar{11}$	34.2	194	35	194
9, 14, $\bar{1}\bar{1}$	34.2	346	34.6	347
14, 5, $\bar{11}$	57.6	49	57	48.6
14, 5, $\bar{1}\bar{1}$	57.6	131	56.2	131
5, $\bar{9}$, $\bar{11}$	73.7		not observed	
5, $\bar{9}$, $\bar{1}\bar{1}$	73.7		not observed	

along the c axis unless one applies only the minimum voltage required for path formation. With caution a trigonal set of paths is obtained which lie within vertical reflection planes that bisect the horizontal coordinate axes and are inclined at 54° to the c axis. The parameters obtained for the trigonal set are [2, 1, 1.45] which, when transformed into Miller indices, become (705), the direction quoted by Kreft and Steinmetz. In oblique sections additional path directions appear; [10, 5, 2] was observed in cleavage sections, and in (010) sections the path sets [2, 1, 1.45] and [110] but not [10, 5, 2] were observed. A correlation between path directions in different oblique sections was not obtained, but in all of them the basal section paths were identified. The path indexing seems to show that the additional paths are contained within reflection planes and that they possess large inclination angles with the c axis which may explain why they are not observed in basal sections. In aragonite (V, 5, C) no additional paths are observed in oblique sections.

B. Quartz (SiO_2) *'18; D_3'* [[*101*]]

The trigonal path set observed in a basal section of quartz (Fig. 15) lies within the vertical planes that contain the horizontal coordinate axes and are inclined at 42° to the c axis. They seem to lie parallel to the intersections of alternate pyramidal faces. Excess voltage applied at room temperature did not produce other paths. In liquid air, however, the paths appear to go straight through. Paths in addition to the trigonal set appear in prismatic sections.

5. Orthorhombic System

The breakdown paths observed in crystals of the orthorhombic system all lie within principal planes as shown schematically in Fig. 16. All the crystals examined belong to the normal symmetry class '8; V_h.'

A. Baryte ($BaSO_4$) [[*0, 9, 11*]], [[*100*]]

Measurements and observations of von Hippel[2] are confirmed. The complete pattern consists of the paths:

[0, 9, 11] [0, $\bar{9}$, 11] [100]

FIG. 15. Trigonal path set in basal quartz.

B. Sulphur (S_{128}) [[*021*]], [[*100*]]

The following path directions were observed at room temperature:

In a (100) section—[100] paths directed straight through.
In a (010) section—symmetrical fork paths in (100) plane and inclining at 47°.
In a (001) section—complimentary forks in (100) plane.
In (110) and (111) sections—[100] paths only (Fig. 17).

Both the tester and the ivory electrode methods were used to produce paths. The [100] or a-paths form more readily than the fork paths as shown by the behavior in (110) and (111) sections. The complete pattern consists of the paths:

[021] [0$\bar{2}$1] [100]

C. Aragonite ($CaCO_3$) [[*670*]] [[*001*]]

The following path directions were observed:

In a (100) section—symmetrical fork paths lying in the (001) plane and inclining at 62°, and [001] surface paths.
In a (010) section—complimentary fork paths inclining at 28° in (001) plane, and surface [001] paths.
In a (001) section—[001] paths through section.
In a (110) section—a single path in the (001) plane at 30° inclination, and surface [001] paths.
In an oblique (0, 2.4, 1) section—three paths observed: one inclining at 60° and the other two constituting a symmetrical oblique fork inclining at 41°.

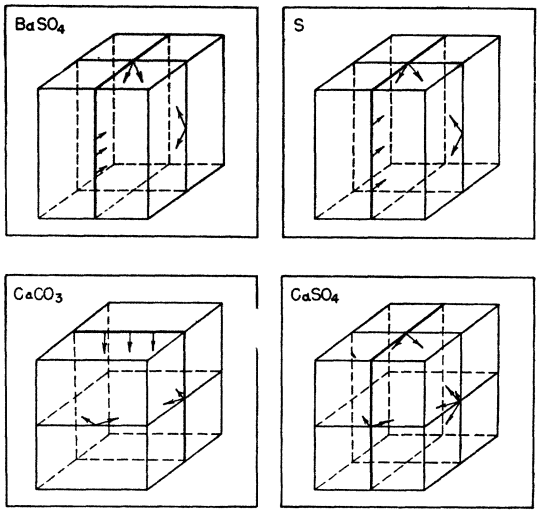

FIG. 16. Breakdown path directions in orthorhombic crystals.

Paths with parameters [670] and [6$\bar{7}$0] should appear as symmetrical forks inclining at 62° and 28° in (100) and (010) sections. They should incline at 30° and 86° in (110) sections, and should also appear as a symmetrical oblique fork inclining at 40.1° in the oblique (0, 2.4, 1) section. The [001] path should incline at 60° in the oblique section. The complete pattern for all orientations of aragonite is, therefore:

[670] [6$\bar{7}$0] [001]

D. Anhydrite ($CaSO_4$) [[*580*]] [[*087*]]

Using the experimental angles obtained by Kreft and Steinmetz[6] for the path directions in anhydrite, the above path parameters are obtained. The pattern is different from those observed in other crystals of this system in that there are two sets of fork paths instead of only one; thus, from a (010) face a path quartet is observed. The four paths in the pattern are the following:

[580] [5$\bar{8}$0] [087] [0$\bar{8}$7]

VI. DISCUSSION OF EXPERIMENTAL RESULTS

The breakdown path directions are not dependent upon the orientation of the crystal relative to the field. The paths in oblique sections of sodium chloride, apophyllite, sulphur, aragonite, and in calcite are in the same directions as in prismatic cuts. The existence of additional path directions in oblique cuts that do not appear in basal sections of crystals such as calcite and quartz does not violate the rule stated above, since these paths possess large inclination angles in the basal section. (V, 4, A, B.)

Breakdown paths obey the laws of macroscopic crystal symmetry; that is, given one path, the orientations of all the remaining paths in the pattern may be predicted from symmetry considerations.

Breakdown paths tend to lie within reflection planes and therefore tend to form degenerate patterns whenever such planes exist. A degenerate pattern, recognized by the presence of zeros or repeated numbers in the path parameters, is one that exhibits fewer allowed path directions than the maximum number of directions permitted by the symmetry class under consideration. For instance, (a) in the isometric system, the sequence of patterns [100]→[111]→[110] →[*xxy*] observed in the alkali halides represents a sequence of decreasing degeneracy. It will be observed (Fig. 12) that all the above directions are contained within (110) reflection planes. The [110] paths observed in fluorite and sphalerite (V, 1, B, C) are contained within (110) reflection planes. In sodium chlorate (V, 1, D) the [552] pattern is non-degenerate since the tetartohedral class possesses only 12 equivalent points and contains no reflection planes. (b) In the tetragonal system, KH_2PO_4 exhibits the non-degenerate patterns [20, 9, 16] and [15, 4, 7] in the absence of reflection planes, whereas apophyllite possesses five reflection planes and shows a degenerate path pattern. (c) In the hexagonal system, beryl with seven reflection planes belongs to the most symmetrical class of this system. The paths, which are directed along the coordinate axes, are the most degenerate possible. Apatite is an exception for it shows a non-degenerate pattern in the presence of a single basal reflection plane (V, 3, B). (d) In the trigonal system, quartz reveals a degenerate set in the absence of reflection planes (V, 4, B). The trigonal set of paths observed in basal sections of calcite (V, 4, A) are degenerate and lie within the only reflection planes that the crystal possesses. In oblique cuts the additional paths that appear seem to lie within these same

reflection planes. A complete indexing of these paths, however, was not carried out. (e) In the orthorhombic system, the paths in every instance were observed to lie within reflection planes (V, 5, A, B, C, D).

The type of lattice bond does not seem to influence the path patterns in a characteristic way. The path pattern observed in sulphur (V, 5, B), a crystal that exhibits covalent and molecular bonding, is similar to the patterns observed in aragonite and baryte (V, 5, A, C) which are essentially ionic in nature, but belong to the same symmetry class.

The breakdown path directions do not appear to be related in a directly obvious manner to the atomic positions in the lattice. This is most convincingly demonstrated by the path patterns observed in sulphur (V, 5, B). The structure, as shown by Warren and Burwell,[12] is similar in appearance in the (a) and (b) directions and is quite different in the (c) or [001] direction. Looking at the structure from (a) or (b) one observes lines of sulphur rings extending diagonally through the crystal at *ca.*±45° to the line of sight in the [110] and [1$\bar{1}$0] directions, i.e., parallel to the base. The lines are not meshed; thus, in one layer the lines all run in the [110] direction, in the next [1$\bar{1}$0], etc. Each ring, which consists of 8 sulphur atoms, stands on end in the (c) direction and faces *ca.*±45° to the observer at (a) or (b). From (c) one views the sulphur rings end-on; thus, the structure looks different and more open.

On the basis of the structure one might expect similar patterns for (100) and (010) cuts, and a different one for (001). Furthermore, the existence of the 45° line of sulphur rings might lead to the prediction of the following pattern.

In a (100) section—symmetrical fork paths inclining at 45° and lying in the (001) plane.
In a (010) section—complimentary fork paths in the (001) plane.
In a (001) section—[001] paths through sample.

This does not agree with the pattern observed which in (010) and (001) cuts shows symmetrical fork paths at approximately±45° lying in the (100) plane and [100] paths in (100) and oblique sections.

In the alkali halides the sequence of path patterns observed suggests that the path directions may change according to the sequence of decreasing interplanar distances, but the [111] paths seem to be out of position, and the parameters of the star paths do not fit closely to the scheme. Further investigation, however, may show more conformity.

VII. CONCLUSIONS

Before considering a mechanism for breakdown path orientation one should be familiar with related electronic phenomena in crystals. A review of pertinent information has recently been presented by von Hippel[13] who discusses the problem of breakdown path orientation in the frame of his general theory on the breakdown of solid dielectrics. The mechanism which he has evolved is based on the assumption that the

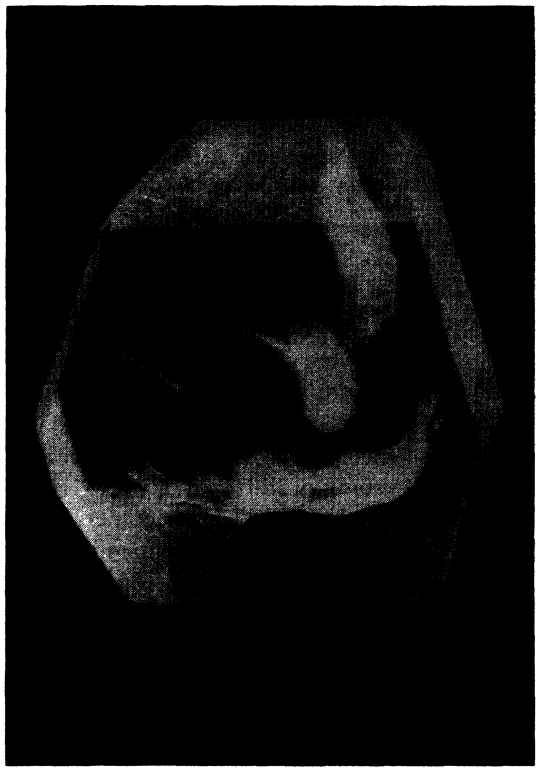

FIG. 17. [100] paths in (111) sulphur at 20°C paths appear double due to refraction.

[12] B. E. Warren and J. T. Burwell, J. Chem. Phys. **3**, 6 (1935).

[13] A. von Hippel, Proc. Faraday Soc., Conference on Dielectrics, Bristol, 1946.

paths mark directions for which there is least transfer of energy from excess electrons, which are accelerated by the applied field, to the lattice. The path directions are believed to depend upon the wave-length, and hence upon the velocity of excess electrons. The orientating mechanism proposed by him is electron wave interaction with the lattice that results in scattering into preferential lattice directions.

The experimental foundation for an exact theory, however, is not yet complete. We are working further on this problem.

ACKNOWLEDGMENT

The author wishes to thank Professor Arthur von Hippel for the use of his personal equipment and mineral collection as well as for his help and encouragement throughout this investigation.

PHYSICAL REVIEW VOLUME 70, NUMBERS 9 AND 10 NOVEMBER 1 AND 15, 1946

The System of Microstresses in Cold-Worked Metal

NELSON M. BLACHMAN*
Case School of Applied Science, Cleveland, Ohio
(Received July 1, 1946)

Smith and Stickley have measured the x-ray line widths from specimens of cold-worked α-brass and tungsten as functions of Bragg angle and x-ray wave-length. Their results accord with the microstress theory of broadening. They find that with α-brass, which is elastically anisotropic, the line width depends upon crystallographic direction in a systematic manner, while with tungsten, which is elastically isotropic, it does not. For several very simple theoretical models of internal-stress systems the variation in line width with crystallographic direction is computed here. The one which fits the above results best, though poorly, is that which assumes that the homogeneously strained domains suffer uniform normal stress of random magnitude. A plausible model for the microstress system and a very good fit are obtained by superposing upon this model any of the other models considered and thus obtaining the proper amount of anisotropy.

INTRODUCTION

CONSIDERABLE attention has been given in the last twenty-five years to the generally observed broadening of the x-ray diffraction lines of polycrystalline metal by cold work. The microstress theory of x-ray line broadening assumes a system of internal stresses (microstresses) in a piece of cold-worked metal which are in some manner random in magnitude and direction and are constant only over domains very small compared with the sample. If we apply Bragg's law, $\lambda = 2d_{hkl} \sin \theta_{hkl}$, to one of these homogeneously stressed and, therefore, homogeneously strained domains, we find upon logarithmic differentiation, taking λ constant, the following relation between the microstrain $e_{hkl} = \Delta d_{hkl}/d_{hkl}$ in the direction normal to the (hkl) planes and the angular displacement of the hkl reflection to which it gives rise,

$$\Delta\theta_{hkl} = -e_{hkl} \tan \theta_{hkl}.$$

The displaced reflections coming from all the various crystallites which are in position to reflect combine to form a broadened line, in which the root-mean-square displacement of the Bragg angle is evidently $\tan \theta_{hkl}$ times the r.m.s. value of e_{hkl}, which we shall denote by E_{hkl}.

Smith and Stickley find $B_{hkl}/\tan \theta_{hkl}$ (B = corrected half-intensity breadth of line) to be independent of λ, in agreement with this prediction of the microstress theory.[1] With cold-worked tungsten, which is elastically isotropic, they found it also independent of crystallographic direction, but not with α-brass, which is elasti-

* Now at Cruft Laboratory, Harvard University, Cambridge, Massachusetts.

[1] Charles S. Smith and E. E. Stickley, Phys. Rev. 64, 191 (1943).

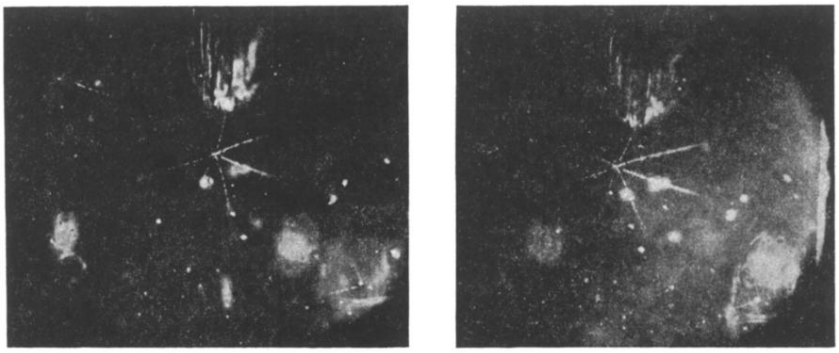

FIG. 11. [133] star LiF 150°C.

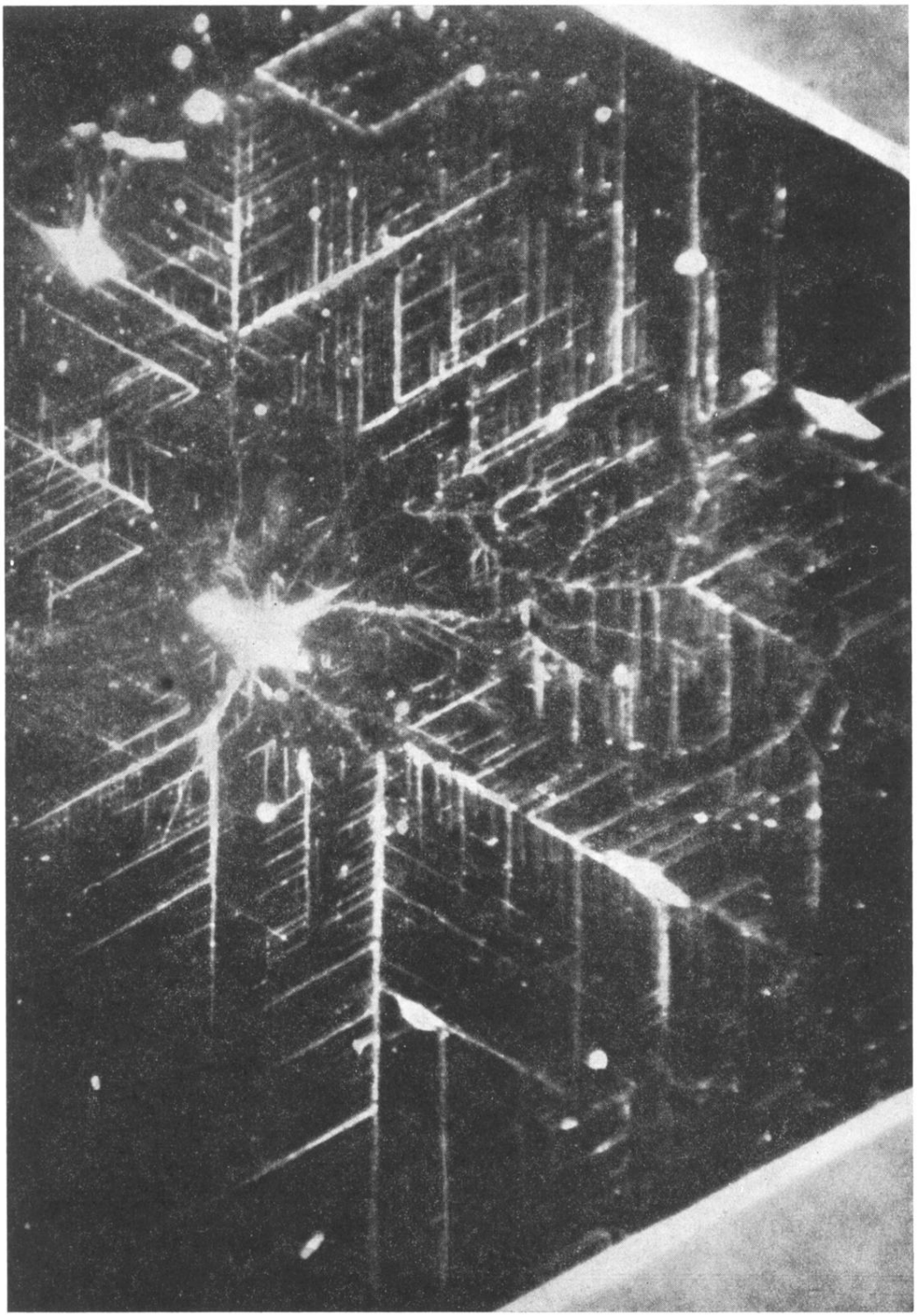

FIG. 13. [110] surface breakdown paths on (111) fluorite.

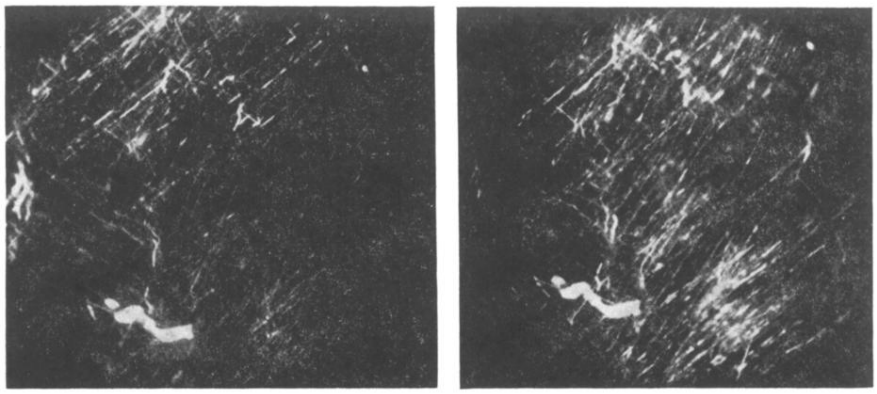

FIG. 14. Pattern in (100) KH_2PO_4.

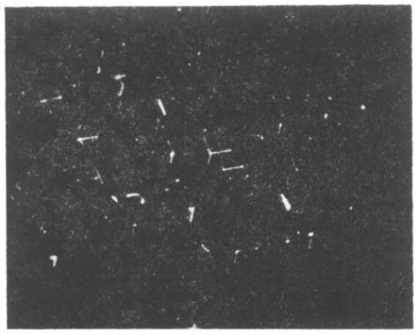

FIG. 15. Trigonal path set in basal quartz.

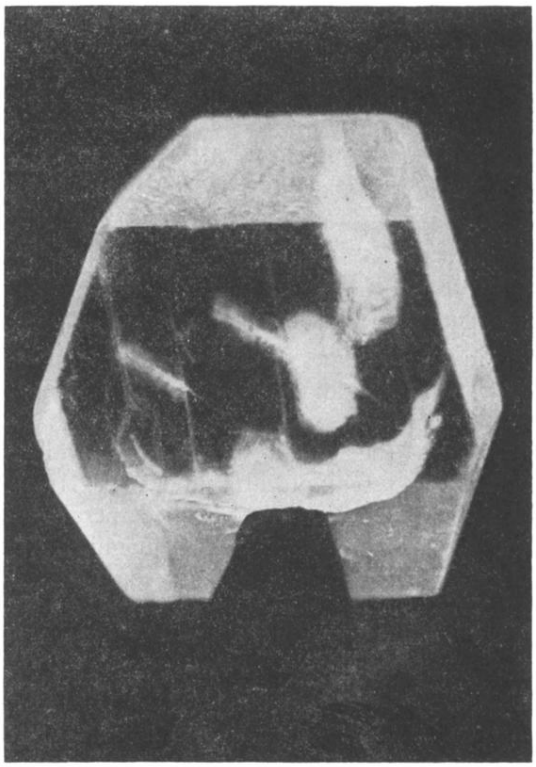

FIG. 17. [100] paths in (111) sulphur at 20°C paths appear double due to refraction.

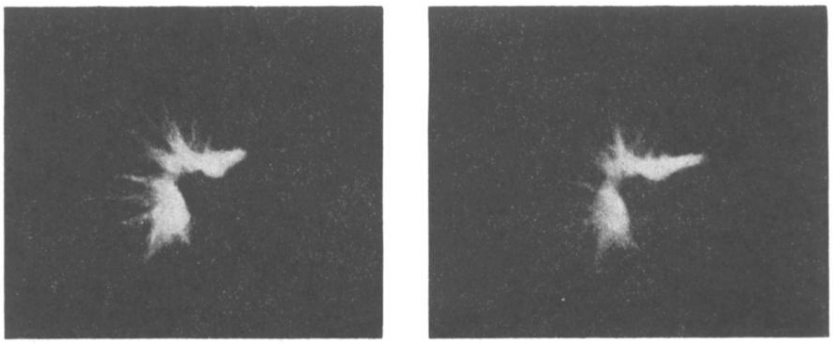

FIG. 4. Random RbBr −180°C.

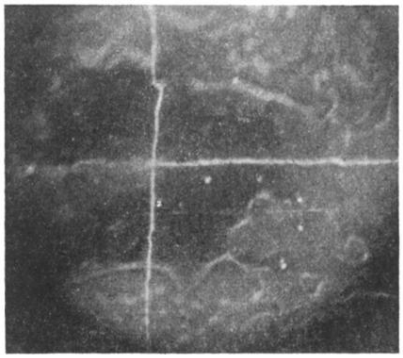

FIG. 5. [100] (100) RbBr 20°C.

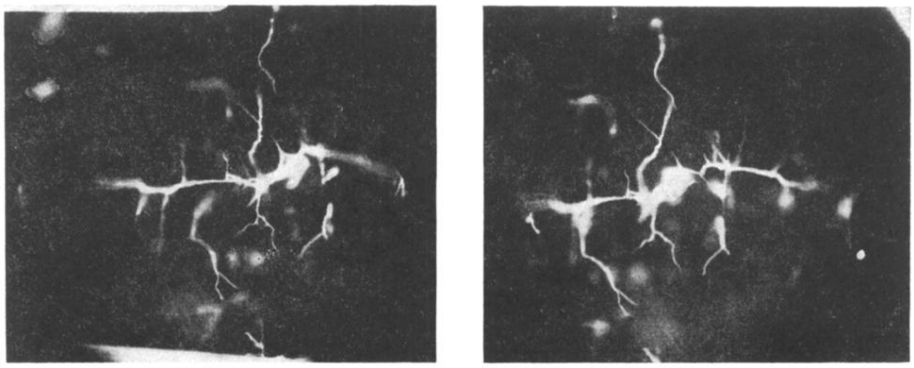

FIG. 6. [100] & R in (110) NaCl at $-180°C$.

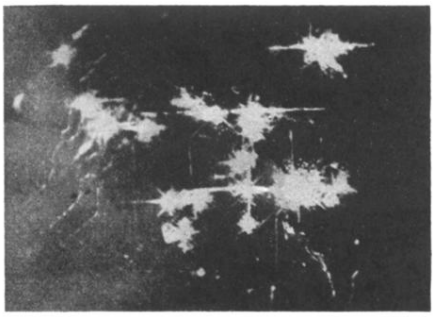

FIG. 7. [100] thin (100) NaCl at −180°C overvoltage.

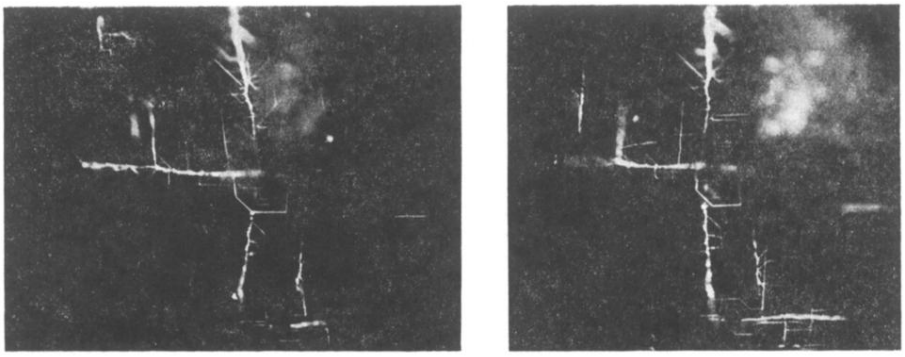

FIG. 8. [110] (100) NaCl 20°C.

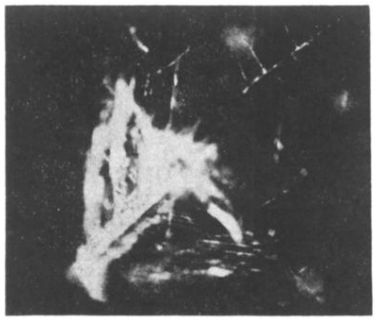

FIG. 9. [111] thin (100) NaCl at 20°C overvoltages.